Molecular Biology of the Cell
Vol. 12, 2534–2545, August 2001

Actin Polymerization Is Essential for Pollen Tube Growth[V]

Luis Vidali,*† Sylvester T. McKenna,‡ and Peter K. Hepler†

†Biology Department, Molecular and Cellular Biology Program, University of Massachusetts, Amherst, Massachusetts 01003; ‡Biology Department, Long Island University, Brooklyn, New York 11201

Submitted December 7, 2000; Revised April 17, 2001; Accepted June 11, 2001
Monitoring Editor: Thomas D. Pollard

Actin microfilaments, which are prominent in pollen tubes, have been implicated in the growth process; however, their mechanism of action is not well understood. In the present work we have used profilin and DNAse I injections, as well as latrunculin B and cytochalasin D treatments, under quantitatively controlled conditions, to perturb actin microfilament structure and assembly in an attempt to answer this question. We found that a ~50% increase in the total profilin pool was necessary to half-maximally inhibit pollen tube growth, whereas a ~100% increase was necessary for half-maximal inhibition of cytoplasmic streaming. DNAse I showed a similar inhibitory activity but with a threefold more pronounced effect on growth than streaming. Latrunculin B, at only 1–4 nM in the growth medium, has a similar proportion of inhibition of growth over streaming to that of profilin. The fact that tip growth is more sensitive than streaming to the inhibitory substances and that there is no correlation between streaming and growth rates suggests that tip growth requires actin assembly in a process independent of cytoplasmic streaming.

INTRODUCTION

Pollen tube growth delivers the sperm to the ovule in higher plants and is thus essential for sexual reproduction. The process is highly polarized, fast, and dependent on the actin cytoskeleton (Franke *et al.*, 1972; Mascarenhas and Lafountain, 1972; Steer and Steer, 1989; Derksen *et al.*, 1995; Taylor and Hepler, 1997), although the mechanism is still controversial (Vidali and Hepler, 2000). Long parallel bundles of F-actin occur along the shank of the pollen tube (Perdue and Parthasarathy, 1985; Lancelle *et al.*, 1987; Lancelle and Hepler, 1992), but these become disorganized close to the cell apex, where a loose meshwork with diminishing amounts of F-actin reside (Lancelle *et al.*, 1987; Heslop-Harrison and Heslop-Harrison, 1991; Miller *et al.*, 1996; Kost *et al.*, 1998). In tobacco pollen tubes this disorganized region sometimes contains a "ring" or "collar" of bundled microfilaments, as revealed by a GFP fusion of the F-actin binding domain of talin (Kost *et al.*, 1998). The disorganized region also corresponds to the well-known apical clear zone of the pollen tube described by light and electron microscopy (Heslop-Harrison and Heslop-Harrison, 1990; Lancelle and Hepler, 1992), which is also occupied by mitochondria, dictyosomes, secretory vesicles, and ER. In the shank of the pollen tube, larger organelles (amyloplasts, vacuoles), together with the aforementioned organelles and secretory vesicles, undergo rapid bidirectional cytoplasmic streaming, being driven by acto-myosin (Shimmen and Yokota, 1994).

Different mechanisms can be envisioned for the participation of the actin cytoskeleton in pollen tube elongation. The first and most parsimonious explanation is that actin bundles control cytoplasmic streaming and hence the delivery of secretory vesicles essential for growth (Mascarenhas and Lafountain, 1972; Mascarenhas, 1993; Taylor and Hepler, 1997; Kost *et al.*, 1998; Geitmann and Emons, 2000). Therefore, the inhibition of this actin system would stop growth because of the interdiction of vesicle transport. An alternative explanation could be that, in addition to actomyosin-driven streaming, actin polymerization itself participates in the elongation process, either as a force generator or as an organizer of the apical cytoplasm (Picton and Steer, 1982; Vidali and Hepler, 2001). The first hypothesis predicts that pollen tube growth would be correlated to cytoplasmic streaming rates and that the effects of inhibitors would be equivalent in both streaming and growth, as indicated in the initial observations of Mascarenhas and Lafountain (1972). However, recent studies, which suggest that growth can be uncoupled from cytoplasmic streaming (Lin and Yang, 1997; Gibbon *et al.*, 1999; Miller *et al.*, 1999; Geitmann *et al.*, 2000), demand that these earlier observations be reevaluated. Based on what is known today about the participation of actin in cellular motility (Pollard *et al.*, 2000), a more current view would hold that actin polymerization could drive pollen tube elongation. If this hypothesis is correct, actin polymerization should be correlated with pollen tube elongation, whereas cytoplasmic streaming should be independent.

[V] Online version of this article contains video material for Figures 7 and 9. Online version is available at www.molbiolcell.org.

* Corresponding author. E-mail address: lvidali@bio.umass.edu.

Abbreviations used: DIC, differential interference *c*ontrast; PLP, poly-L-proline, rh-dextran, rhodamine-dextran.

Although qualitative results indicate that pollen tube growth is more sensitive to actin inhibitors than cytoplasmic streaming (Gibbon *et al.*, 1999; Geitmann *et al.*, 2000), we have applied a more stringent, quantitative assessment of this problem. In addition to finding no correlation between growth and streaming rates in untreated pollen tubes, we show growth to be two to six times more sensitive than streaming to actin-disrupting agents. Our results suggest that actin directly participates in the pollen tube growth process independently of cytoplasmic streaming, with actin polymerization being a rate-limiting step for pollen tube elongation.

MATERIALS AND METHODS

Cell Culture

Pollen from *Lilium logiflorum* was hydrated and grown in pollen growth medium (PGM) composed of 15 mM MES, 1.6 mM BO_3H, 1 mM KCl, 0.1 mM $CaCl_2$, 7% sucrose, pH 5.5. After 1.5–2 h, pollen tubes were immobilized with low melting point agarose (Sigma, St. Louis, MO), final concentration 0.7%, and allowed to recover for 15 min. Those that were growing vigorously were selected for microinjection. Latrunculin B (Calbiochem, La Jolla, CA) and cytochalasin D (Boehringer Mannheim, Indianapolis, IN) were resuspended in the containers supplied by the manufacturer to a 2.5 mM stock in DMSO and then diluted to the appropriate concentration in PGM. For latrunculin B or cytochalasin D treatment, after cells had recovered from plating, the medium was exchanged twice with the desired concentration of inhibitor to avoid dilution and to ensure the correct final concentration. For control cells, the medium was exchanged with fresh PGM.

Protein Purification

Pollen profilin was purified as reported previously with minor modifications (Vidali and Hepler, 1997). Briefly, 5–10 g of dry pollen from *L. longiflorum* were hydrated, filtered, resuspended in extraction buffer (30 mM PIPES, pH 7.0, 250 mM sucrose, 10 mM EGTA, 6 mM $MgCl_2$, 5 mM DTT, 0.8% casein, 1 μg/ml each leupeptin, pepstatin, and aprotonin, 1 mM PMSF), and disrupted with a glass-Teflon homogenizer with 10 strokes at full power. The extract was clarified at 30,000 $\times$ *g* for 15 min, lipids were skimmed, and the extract was further centrifuged at 150,000 $\times$ *g* for 30 min. The supernatant was loaded to a 2.5 $\times$ 5-cm column of poly-L-proline (PLP) MW 30,000 bound to Sepharose-6MB (Sigma). The column was first washed with column buffer (100 mM KCl, 10 mM Tris-HCl, 1 mM DTT, pH 8), then with 2 M urea in column buffer, and finally eluted with 100 ml of 6 M urea in column buffer. The eluant was dialyzed against folding buffer (100 mM KCl, 5 mM DTT, 10 mM Tris-HCl, pH 8) overnight and concentrated by chromatography in a 1 $\times$ 20-cm column of DEAE-Sepharose fast flow (Pharmacia, Piscataway, NJ) and eluted with 0.5 M KCl. The protein was further concentrated, and the buffer was exchanged to injection buffer (2 mM HEPES, 100 mM KCl, pH 7) by Centricon ultraconcentrators (MWC 10,000; Amicon, Beverly, MA). The final protein concentration was 30 mg/ml, which was diluted in injection buffer.

Human profilin 1 was purified according to Fedorov *et al.* (1994) with minor modifications. *Escherichia coli* BL21(DE3) overexpressing human profilin 1 was grown in 4 liters of Luria broth medium at 37°C to 0.6 OD_{600}. Isopropyl-thio-β-D-galactopyranoside was added to 1 mM, and the cells were cultured for 4 h, after which the cells were centrifuged and resuspended in extraction buffer (100 mM KCl, 20 mM Tris-HCl, 1 mM DTT, 1 mM PMSF, pH 8). The suspension was French pressed at 10,000 PSI and centrifuged at 150,000 $\times$ *g* for 1 h. The supernatant was loaded to a 2.5 $\times$ 5 poly-L-proline column that had been equilibrated in column buffer (extraction buffer without PMSF). The column was washed with column buffer and then with 3 M urea and finally was eluted with 6 M urea. The first fractions contained >95% profilin and did not require further purification. The protein was refolded in folding buffer by dialysis overnight. It was further ultraconcentrated to 10 mg/ml and exchanged into injection buffer.

DNAse I grade II was obtained commercially (Boehringer Mannheim) and dissolved in injection buffer. Protein concentration was determined with the Bio-Rad (Hercules, CA) protein assay with the use of immunoglobulin as standard.

Data Acquisition and Analysis

Cells were visualized with differential interference contrast (DIC) optics and a 40$\times$ oil immersion lens, N.A. 1.3 (Nikon, Melville, NY). Images were acquired with cooled charged-coupled device (CCD) cameras from Photometrics (Tucson, AZ) or Roper Scientific (Tucson, AZ), with either a 0.29- or a 0.08-μm/pixel resolution, respectively. The low-resolution camera was driven by the PMIS software (Photometrics), which allows for macro programming, and the high resolution one by MetaMorph software (Universal Imaging, West Chester, PA) with the use of predesigned algorithms for image acquisition and particle tracking. All images were obtained at 12 bit. Cells were illuminated with 540-nm (green) light; to remove infrared light, a low-pass, 610-nm filter was used just before the CCD camera. Selected cells were imaged for 10 frames, 4 s apart, and then for 20 frames, 0.6 s apart. The cells were microinjected with different concentrations and amounts of either buffer + 0.5 mg/ml rhodamine-dextran MW 10,000 (rh-dextran, Molecular Probes, Eugene, OR) or buffer + 0.5 mg/ml rh-dextran with any of the following: BSA, casein, pollen profilin, human profilin 1, or DNAse I. After 10 and 20 min, 20 frames were collected 4 s apart, and 20 more frames were collected 0.6 s apart. After the last frame, a fluorescent image was recorded with the use of the rhodamine filter set. Finally, a DIC background image was taken by moving the cell out of the field of view.

Images were background subtracted and exported as 8-bit files to the TIFF format. Stacks were recovered with the NIH-image software running on a Macintosh emulator (Executor, ARD1, Alburquerque, NM) on a 166 MHz Pentium processor. Macros were written in NIH-image for automatic measuring of growth and cytoplasmic streaming. Growth was measured by tracking the highly refractile tip of the pollen tube, which creates a distinct minimum when a line is scanned along the center of the tube. The position of the tip was tracked over the 10 or 20 frames acquired every 4 s. The position vs. time data were exported to the program Microcal Origin (Microcal Software, Northampton, MA) and fitted to a line that always gave *R* values above 0.99. The slope of the line was taken as the pollen tube average growth rate. To determine cytoplasmic streaming rates, the sequences were displayed as a stack with NIH-image. The stack was shadowed to the North-West direction, creating an enhanced contrast of the large organelles, and the image was then thresholded and binarized. The trajectory of single organelles was not trackable over a long period, but an estimate of overall cytoplasmic movement with statistical significance was obtained that closely matched that of a subset of organelles tracked by hand. Frames 1.2 s apart were compared. The location of a particle was determined, and the distance against all detected particles in the next frame was calculated. The position of the closest particle was selected as the new position after 1.2 s. All detectable particles were analyzed in this way. The same pair analysis was performed with a total of 20 frames. Between 300 and 600 displacements were consistently obtained. Rates were exported to Microcal Origin, and histograms were created to display the frequency distribution of rates. The histogram was fitted with a Gaussian function, and its maximum was used as the average cytoplasmic streaming rate.

For some of the latrunculin B and cytochalasin D treatments, the automatic "track objects" function from the software MetaMorph was used to measure cytoplasmic streaming and growth rates; comparable results were obtained between the previously outlined

method and the commercial software. Cells were treated for 20 min with different concentrations of latrunculin B or cytochalasin D in culture medium, and 100 images were acquired at ~0.2-s intervals. Average growth and streaming rates were obtained for 10 control cells, and the mean value used to estimate fractional inhibition of the treated cells.

Determination of the Injectate Concentration

Injections were performed as previously described (Vidali and Hepler, 1997), but rh-dextran MW 10,000 (Molecular Probes) was included in the injection buffer at 0.5 mg/ml. A fluorescent image was used to estimate the volume of injectate delivered into the cell. A region of interest was selected around the pollen tube, and its fluorescence average was determined. The value was compared against a standard curve constructed with flat microcapillaries (Vitro, Rockaway, NJ) with a 20-μm path length. Different concentrations of rh-dextran (5–100 μg/ml) in injection buffer + 100 mM DTT (as an antifade) were loaded in the flat microcapillaries. Exposure time was always 100 ms for cells and standards. The calibration curve was linear in the range of 5–100 μg/ml. Because the images were acquired with a 12-bit camera, saturation was never a problem, and small and large injections could be analyzed with the same exposure time and standard curve. Knowing the concentration of injectate in the needle and its dilution relationship to rh-dextran, together with information on the thickness of the cell (18 μm) and its accessible volume (80%; Vidali and Hepler, 1997), it was possible to estimate the concentration in the cell of the injected protein.

Curve Fitting and Statistical Analysis

Plots of inhibitor concentration vs. inhibition showed a very steep dependence on the concentration of the inhibitor. For microinjected cells, values obtained 10 and 20 min after injection and having a similar intracellular concentration were averaged both for fractional inhibition and intracellular concentration. Each data point on the graphs in Figure 2 represent 3 or 4 cells. For inhibitor treated cells, values from 9 to 10 cells were averaged. To calculate half-maximal inhibitory concentration (IC_{50}) a logistic regression model, weighted for the error of the data, was used. The nonlinear fitting function of the program Microcal Origin, which is based on the minimization of χ^2 by the Levenberg-Marquardt algorithm, was used. Because the precise mechanism of inhibition is probably complex, we only use this model as a geometrical tool to calculate IC_{50}. Multiple curves were compared by a double-tailed *t* test of the resultant IC_{50}; values of $p < 0.05$ were taken as statistically significant.

Actin Staining

F-actin was detected with Alexa-phalloidin (Molecular Probes) with an adaptation to the protocol of Doris and Steer (1996). Twenty minutes after profilin injection or latrunculin B treatment, the cells were cross-linked with 300 μM *m*-maleimidobenzoyl-*N*-hydroxysuccinimide ester (MBS; Pierce, Rockford, IL) and 300 μM disuccinimidyl suberate (DSS; Pierce) for 15 min at room temperature in PGM with 9% sucrose instead of 7%. The cells were then fixed with 3.7% formaldehyde and 0.1% glutaraldehyde in fixation buffer (100 mM PIPES, 10 mM $MgCl_2$, 0.1% NaN_3, pH 6.8) for 30 min and thereafter were treated with staining buffer (fixation buffer + 0.1% Triton X-100 + 0.3 μM Alexa-phalloidin; Molecular Probes) for 1 h. After three washes with washing buffer (fixation buffer + 0.1% Triton X-100 + 1 mg/ml *p*-phenylenediamine), cells were observed with the confocal microscope MRC-600 (Bio-Rad). Optical sections (n = 10–30) were acquired at 1- or 0.5-μm intervals in the Z-axis. Three dimensional (3D) reconstructions and maximal projections were performed with MetaMorph.

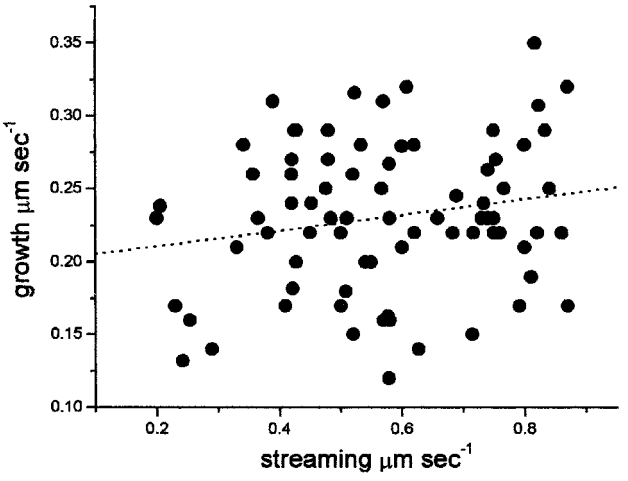

Figure 1. Cytoplasmic streaming rates are not correlated with pollen tube growth rates. Growth and streaming rates were determined automatically by computer algorithms. The value for growth is the average over a 40-s interval from digital images acquired with a CCD camera. Streaming rates were calculated from more than 400 particle displacements per pollen tube. From all the observed pollen tubes the average growth rate was 0.23 ± 0.05 μm/s, and the average streaming rate was 0.57 ± 0.17 μm/s. The lack of correlation between the two parameters is clear from the line fitting, which was obtained by least squares; $R^2 = 0.034$, p = 0.1, n = 78.

RESULTS

Pollen Tube Growth Rates and Cytoplasmic Streaming Rates Are Not Correlated

To evaluate the participation of the actin cytoskeleton in pollen tube growth, we initially focused on the dependence of growth on cytoplasmic streaming. By using a combination of digital image filtration and multiple particle tracking, we have automated this complicated process. The developed algorithm allowed us to determine total particle displacement in two consecutive DIC images acquired 1.2 s apart for large data sets (see MATERIALS AND METHODS). Figure 1 was generated by >25,000 measured particle displacements, with an average cytoplasmic streaming rate in pollen tubes of 0.57 ± 0.17 μm/s. The observed organelles never reached speeds faster than 2 μm/s, which is in close agreement with recently reported values for pollen tubes (de Win, 1997). The average growth rate that was measured for 78 pollen tubes was 0.23 ± 0.05 μm/s. Although the average streaming rate among different tubes varied from 0.2 to 0.9 μm/s and the average growth rate varied from 0.10 to 0.35 μm/s, we found no correlation between these two rates ($R^2 = 0.034$, p = 0.1, n = 78; Figure 1).

Increasing the Intracellular Pool of Profilin Inhibits Pollen Tube Growth and, to a Lesser Extent, Cytoplasmic Streaming

The lack of correlation between growth and streaming rates prompted us to investigate in detail the participation of the actin cytoskeleton in pollen tube growth. The most abun-

dant actin-binding protein in pollen is profilin, which is thought to block spontaneous nucleation and maintain a pool of monomeric actin ready for polymerization at activation sites (Pollard *et al.*, 2000). Profilin has been shown to disrupt the actin cyto-architecture in plant cells when injected at high concentrations (Staiger *et al.*, 1994; Valster *et al.*, 1997). Here, we have increased the intracellular concentration of profilin in a controlled way. To estimate the final concentration of the injected protein, rh-dextran (MW 10,000) was included in the injection buffer. The final concentration of protein was extrapolated from the dilution factor of the injected dextran as estimated by fluorescence (see MATERIALS AND METHODS). We injected buffer, rh-dextran, and control proteins at different concentrations as a control for the injection process and analyzed their effects on pollen tube growth and cytoplasmic streaming. Sometimes the injection process causes a brief inhibition of growth for 2–3 min, but it is completely reversible, and impressively, the majority of the cells recover to identical growing rates as before injection. Cytoplasmic streaming does not show any differences in rates and remains constant during the time analyzed.

We found that increasing the intracellular concentration of profilin in pollen tubes has an important and dramatic effect on pollen tube growth and a substantial but less dramatic effect on cytoplasmic streaming (Figure 2A). Because the major effect of profilin is on F-actin nucleation, this result suggests that F-actin nucleation and likely subsequent actin polymerization are participating in pollen tube elongation. Pollen tubes growing undisturbed have an almost identical morphology between them (Figures 3-5, left panels, and 7A). Close inspection of the morphology of the profilin-injected cells shows clear differences from that of the controls. In the partially inhibited cells the clear zone is reduced (Figure 3, A–C) and is completely absent in nongrowing tubes (Figure 3D). Interestingly, the tubes that were still elongating became thinner in diameter, and the direction of growth was erratic (Figure 3, B and C), suggesting that actin polymerization can regulate not only the speed of growth but also cell diameter and direction. The growth and streaming inhibitions (Figure 2B), as well as the morphological changes (Figure 4) are indistinguishable between pollen profilin and recombinant human profilin 1. Although human profilin 1 and native pollen profilins have different affinities for actin (Gibbon *et al.*, 1997; Kovar *et al.*, 2000), their differences are too small to be detected by live cell assays such as the one used here or in *Tradescantia* stamen hair cells (Gibbon *et al.*, 1997).

The ability to calculate the concentration of profilin necessary to inhibit growth or streaming allowed us to compare it with the intracellular concentration of profilin, which has been previously estimated at 31 μM in these same pollen tubes (Vidali and Hepler, 1997). The calculations show that it is necessary to elevate the total intracellular concentration of profilin by 50% to half-maximally inhibit growth, whereas a doubling of the intracellular concentration of profilin is necessary to half-maximally inhibit cytoplasmic streaming (Table 1). It is important to mention that the difference between these values is statistically highly significant ($p < 0.01$).

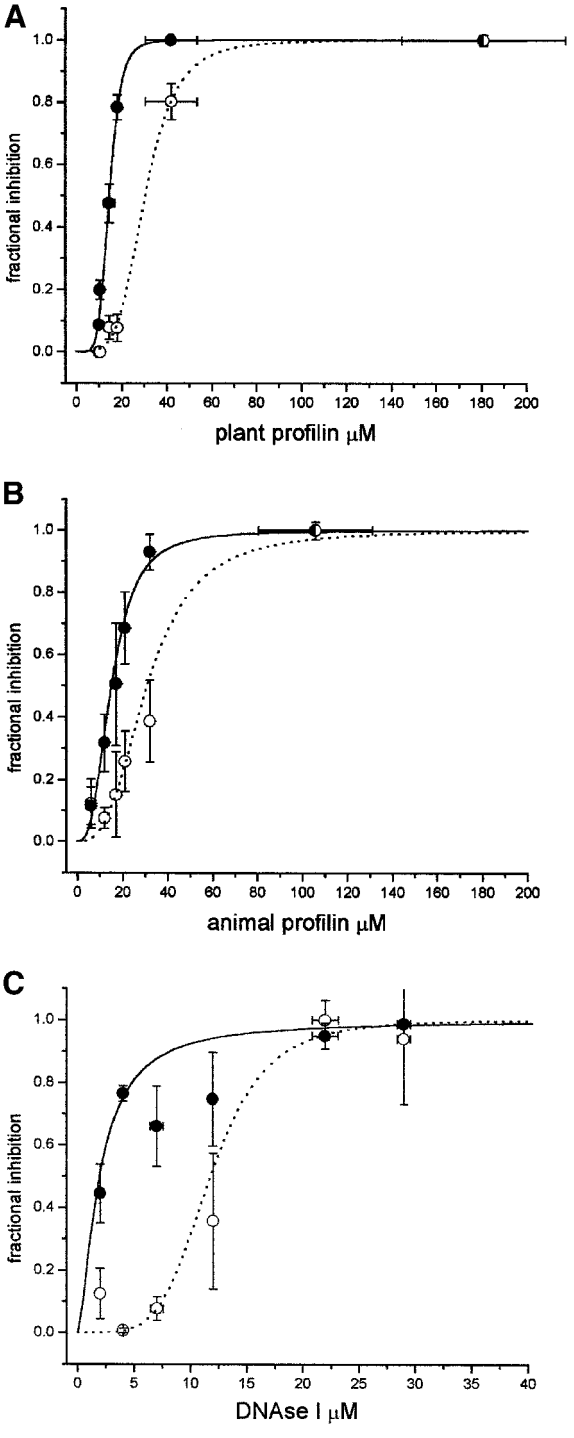

Figure 2. Growth and cytoplasmic streaming inhibition as a function of pollen profilin, human profilin 1, and DNAse I. (A) Inhibition by pollen profilin of growth (●), and cytoplasmic streaming (○). (B) Inhibition by recombinant human profilin 1. (C) Inhibition by DNAse I. The results for three or four cells having a similar intracellular concentration were averaged for both fractional inhibition and concentration; the error bars show the SE of the mean. To calculate the IC_{50}, curves were fitted with a logistic regression model by least squares and weighted for the error of the data.

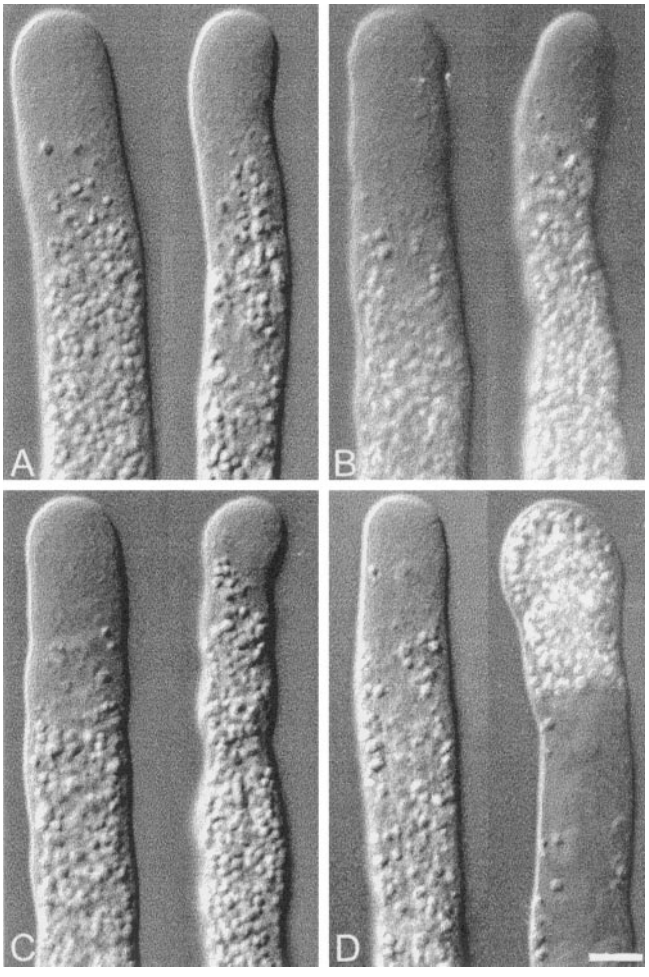

Figure 3. Morphology of pollen tubes injected with increasing doses of native pollen profilin. Leftmost cell of each panel shows the cell before injection, and rightmost 20 min after injection. (A) 10 μM, (B) 16 μM, (C) 22 μM, and (D) 62 μM. Bar, 10 μm. Note the thinning of the cells and erratic growth at low profilin dosages (A–C).

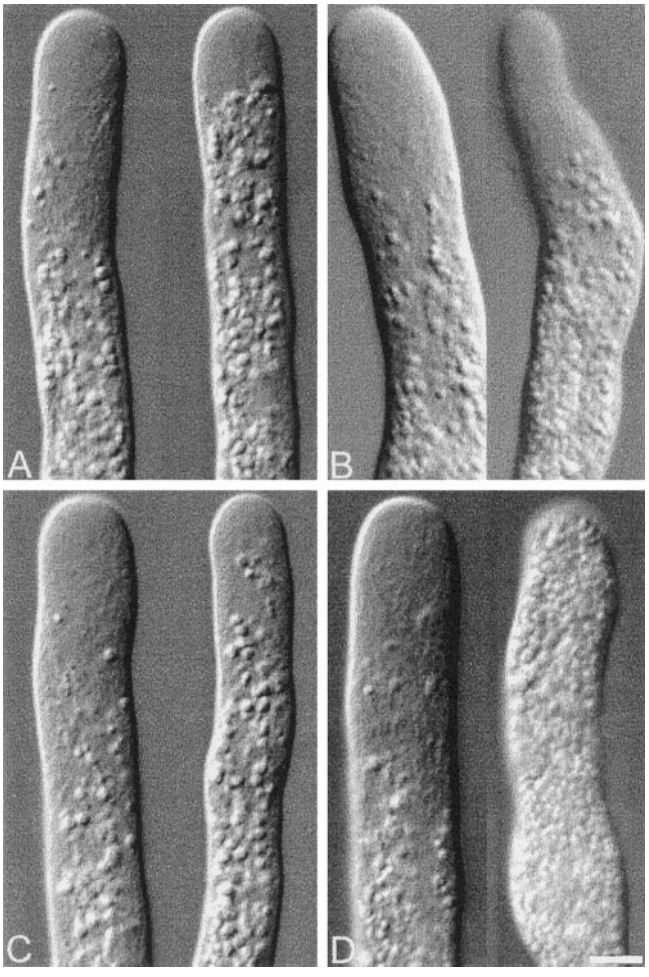

Figure 4. Morphology of pollen tubes injected with increasing doses of recombinant human profilin 1. Leftmost cell of each panel shows the cell before injection, and rightmost 20 min after injection. (A) 10 μM, (B) 18 μM, (C) 22 μM, and (D) 62 μM. Bar, 10 μm. Note the similarity with the morphological changes induced by pollen profilin.

DNAse I Also Inhibits Pollen Tube Growth and Cytoplasmic Streaming but at a Ratio Different From That of Profilin

Because DNAse I has a higher affinity for actin than profilin (Lazarides and Lindberg, 1974; Carter *et al.*, 1997) and because this protein inhibits actin polymerization by a mechanism different from that of profilin (Kabsch *et al.*, 1990), we tested its effects and compared them to those from profilin. Again, pollen tubes were specifically and dose dependently inhibited by DNAse I, but as expected, the IC_{50} values for growth and streaming were lower than those of profilin (Figure 2C and Table 1). Additionally, the proportion of streaming inhibition vs. growth inhibition was remarkably different from that of both profilins, yielding a ratio of 6.2 (Table 1), which is three times higher than that obtained with pollen profilin or human profilin 1. The morphology of the inhibited tubes was similar to the profilin injection in that it generated thinner tubes that grew in an erratic manner (Figure 5, A–D), but the clear zone of the DNAse I–injected cells is more permanent than of those injected with profilin.

Table 1. Summary of the concentration required for half-maximal inhibition of pollen tube elongation and cytoplasmic streaming

	Growth IC_{50}	Streaming IC_{50}	Streaming/ growth
Pollen profilin	14.5 ± 0.4 μM	30.4 ± 1.3 μM	2.09
Human profilin 1	15.0 ± 0.8 μM	30.9 ± 3.6 μM	2.06
DNAse I	1.9 ± 0.4 μM	11.8 ± 1.2 μM	6.21
Latrunculin B	1.7 ± 0.1 nM	3.9 ± 0.4 nM	2.29
Cytochalasin D	207 ± 19 nM	364 ± 27 nM	1.75

Differences between growth and streaming are statistically significant in all cases ($p < 0.01$).

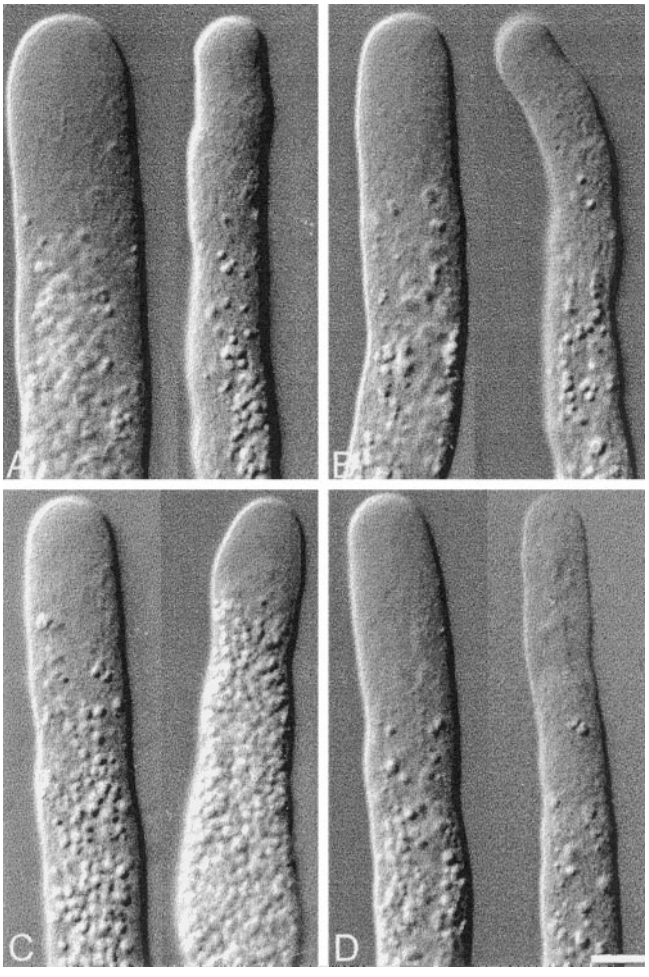

Figure 5. Morphology of pollen tubes injected with increasing doses of DNAse I. Leftmost cell of each panel shows the cell before injection, and rightmost 20 min after injection. (A) 2 μM, (B) 4 μM, (C) 24 μM, and (D) 30 μM. Bar, 10 μm. Note that cell thinning is especially evident.

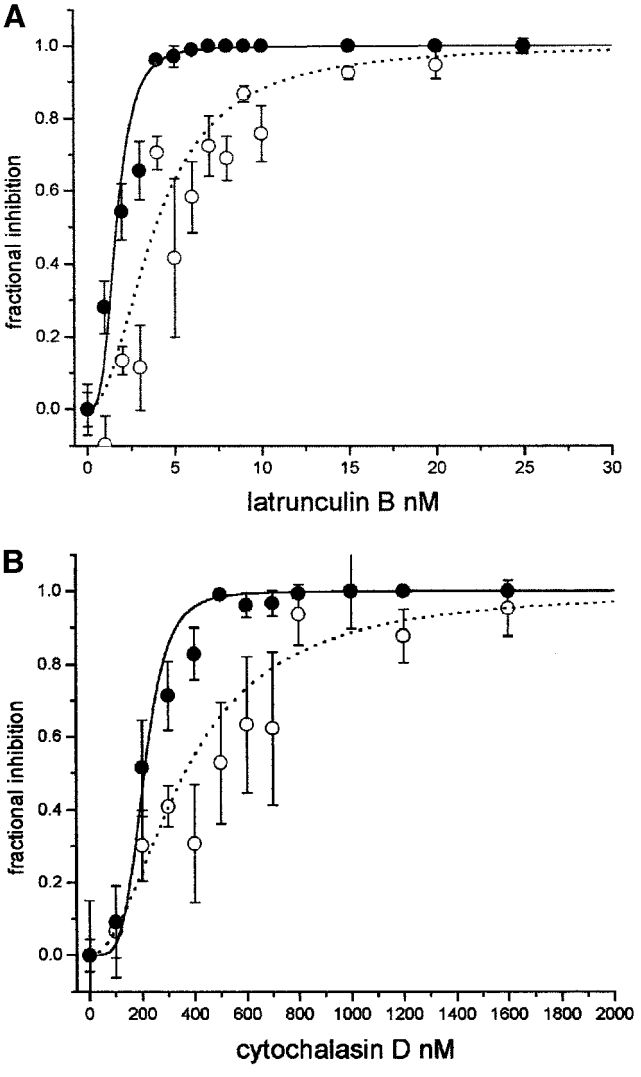

Figure 6. Growth and cytoplasmic streaming inhibition as a function of latrunculin B and cytochalasin D. (A) Latrunculin B dose-dependent inhibition of growth (●) and cytoplasmic streaming (○). (B) Cytochalasin D dose-dependent inhibition. As in Figure 2, to calculate the IC_{50}, curves were fitted with a logistic regression model by least squares. Error bars, SE of the mean from 6–10 cells.

Latrunculin B Inhibits Pollen Tube Growth and Cytoplasmic Streaming at Very Low Concentrations

Latrunculin B has been widely used to disrupt the actin organization in different cellular systems (Schatten *et al.*, 1986; Ayscough *et al.*, 1997; Gupta and Heath, 1997; Oliveira *et al.*, 1997), and its mechanism of action is well understood (Coue *et al.*, 1987; Ayscough *et al.*, 1997; Morton *et al.*, 2000). Here we compared its effects with those of profilin. Extremely low concentrations (1–3 nM) of latrunculin B caused dramatic effects on pollen tube morphology, growth, and streaming. Because the drug does not have to be microinjected, we were able to perform a very detailed analysis of the average growth and streaming rate values from a population of cells treated with different concentrations of the drug. Again, as seen in Figure 6A, we found a stronger inhibition by latrunculin B of pollen tube growth than of cytoplasmic streaming. We determined an IC_{50} of 1.7 ± 0.1 nM for growth and 3.9 ± 0.4 nM for cytoplasmic streaming (Table 1); the ratio of IC_{50} between streaming and growth (~2.3) was also very similar to that of the profilins (~2.0). The morphological alterations induced by latrunculin B are shown in Figure 7. At 1 nM the drug caused a small reduction in the length of the clear zone (Figure 7B, compare with untreated cells in Figure 7A). Increasing the concentration to 2–3 nM resulted in major morphological alterations (Figure 7, C and D); cells had a wavy appearance, some grew thinner, others bifurcated, and only in rare occasions were normal-looking cells observed. At low concentrations, we found a good correlation between the amount of latrunculin B in the medium and the length of the clear zone (data not shown). At 4 nM latrunculin B, cells stop growing and the clear zone was almost abolished (Figure 7E). The morphology of the treated cells was similar to cells injected with high

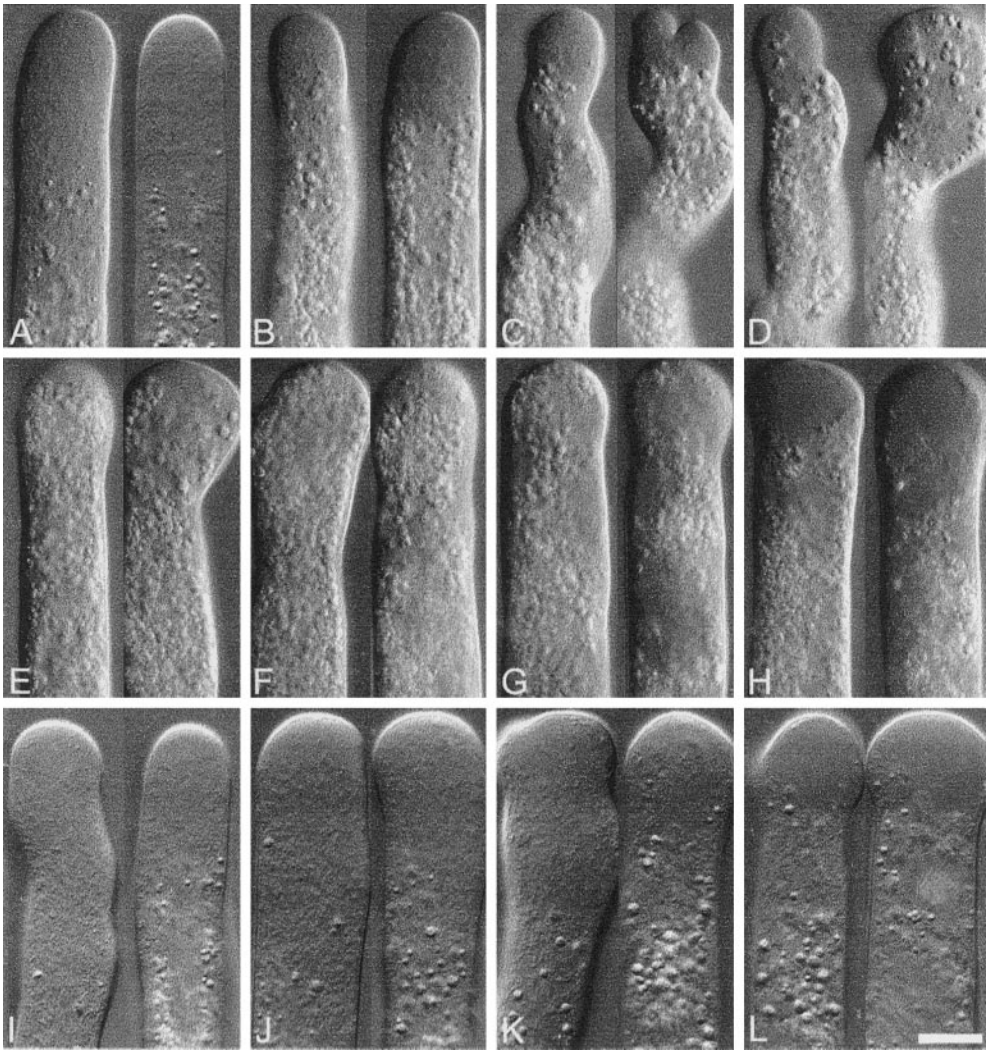

Figure 7. Morphology of pollen tubes treated with increasing doses of latrunculin B or cytochalasin D. (A) Control with no treatment. (B–H) latrunculin B: (B) 1 nM, (C) 2 nM, (D) 3 nM, (E) 4 nM, (F) 8 nM, (G) 15 nM, (H) 25 nM; (I–L) cytochalasin D: (I) 200 nM (J) 400 nM, (K) 800 nM, (L) 1200 nM. Bar, 10 μm. Note the reduction of the clear zone in B; also note the dramatic changes in growth pattern in C and D. The morphology of the cells does not change much between 4 and 15 nM (E–G), but at 25 nM latrunculin B (H) and 1200 nM cytochalasin D (L), the central part of the apical region of the cell becomes smooth, loosing the granularity that characterizes the clear zone. Video files showing the streaming patterns of a control cell (A) and a 3 nM latrunculin B–treated cell (D) are linked to the left image from each pair. (Videos 1 and 2).

profilin concentrations (Figures 3D and 4D). Higher concentrations of latrunculin B did not show additional morphological differences from the 4 nM–treated cells (Figure 7, F and G), until 25 nM was reached (Figure 7H); then the center of the swollen tips became smooth, which is markedly different from the more granular appearance of the clear zone (compare Figure 7, A and H). When the concentration of the drug was increased to 250 nM, most of the cells in the culture chamber burst.

Cytochalasin D Also Shows a Stronger Inhibition of Growth than Cytoplasmic Streaming

Cytochalasin D is a well-known actin-inhibiting drug that at concentrations < 2 μM caps the barbed-end of microfilaments, inhibiting subunit addition and loss from that end (Sampath and Pollard, 1991). This drug had effects very similar to profilin and latrunculin B; it inhibited growth at lower concentrations than streaming, with an IC_{50} ratio of 1.7 (Table 1 and Figure 6B). Interestingly, the morphology of the inhibited cells was slightly different from that of the other inhibitors in that the clear zone was maintained at high inhibitor concentrations (Figure 7, J and K). At very high concentrations, the morphology between the latrunculin B–treated cells and the cytochalasin D–treated cells was similar, although the cells treated with cytochalasin D become more swollen at their tips (compare Figures 7, H and L).

At High Concentrations, Profilin and Latrunculin B Cause a Dose-dependent Disorganization of the Actin Cytoskeleton in Pollen Tubes

To better understand the effect of profilin and latrunculin B in pollen tube growth and streaming, we stained the pollen tube F-actin after profilin injections or latrunculin B treatments, with the use of Alexa-phalloidin as a probe. As can be seen in Figure 8A, growing pollen tubes show a multitude of parallel actin cables that become disorganized close to the tip region. In the subapical region, corresponding to the base of the clear zone, the bundles increase in density and num-

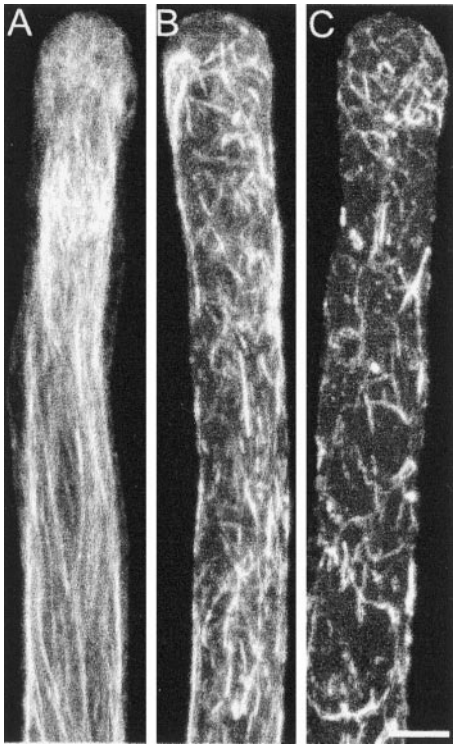

Figure 8. F-actin distribution of profilin-injected cells after chemical fixation and Alexa-phalloidin staining. Twenty minutes after injection cells were chemically fixed and stained with 0.3 μM Alexa-phalloidin. (A) Control cell. (B) Cell injected with a low concentration of profilin (~30 μM). (C) Cell injected with a higher concentration of profilin (>60 μM). All cells were visualized by confocal microscopy; the images are maximal projections of 10 optical sections at 1-μm intervals in the *Z*-axis. Bar, 10 μm.

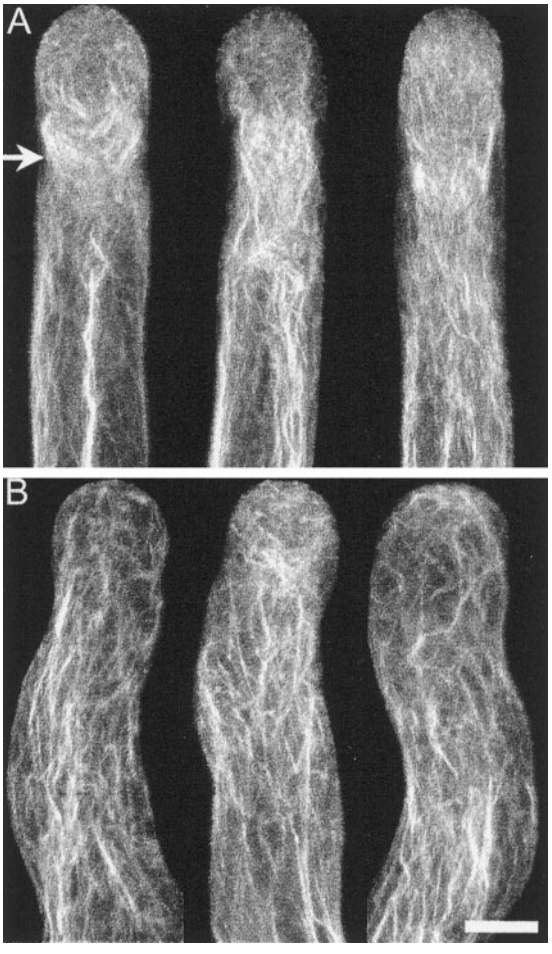

Figure 9. F-actin distribution of cells treated with 2 nM latrunculin B. Treated cells after chemical fixation and Alexa-phalloidin staining. (A) Control cells. (B) Cells treated with 2 nM latrunculin B for 20 min before fixation. F-actin was visualized by confocal microscopy; the images are projections of 30 optical sections at 0.5-μm intervals in the *Z*-axis. There is a video file with a 3-dimensional reconstruction and rotation linked to the first projection from each panel (Videos 3 and 4). Note the prominent subapical funnel-shaped F-actin rich region (arrow in A) that is absent in the treated cells. Bar, 10 μm.

ber, but in the shank of the tube their concentration diminishes again, giving rise to more dispersed actin bundles. The disruption of cytoplasmic streaming can be immediately understood by the changes that occur in the actin cytoskeleton in the shank of the pollen tube. At the profilin dose that causes half-maximal inhibition of streaming (30 μM), a clear disorganization of the microfilament bundles is apparent. They fail to form long bundles and instead, the bundles are fragmented and less axially oriented. In addition, the bundles invade the tip and any polar distribution of the actin is lost (Figure 8B). At concentrations that cause total streaming inhibition (>60 μM) the bundles are scarce and very short, and their orientation is completely lost (Figure 8C). At a higher profilin concentration, the microfilaments are completely absent. Most of the cells that were fixed and stained at high profilin concentration burst, even under optimal conditions.

We also tested the effect of latrunculin B on F-actin. At 25 nM latrunculin B, when cytoplasmic streaming has been completely inhibited, F-actin bundles are still present, but they are not well aligned, and they start to show fragmentation, similar to that seen with profilin at concentrations that inhibit cytoplasmic streaming. At 250 nM, as mentioned before, most cells exploded, but in the few nonruptured cells, the F-actin is present only in short fragments; it was necessary to increase the concentration of latrunculin B to 2.5 μM in order to completely depolymerize the pollen tube F-actin. Similar results have been previously reported (Gibbon *et al.*, 1999; Geitmann *et al.*, 2000).

At Low Concentrations Latrunculin B Causes Only a Change in the Subapical Actin Cytoskeleton and Blocks Growth Oscillations

We analyzed in more detail the structure of the subapical F-actin in cells that were growing erratically, because it was clear that extensive F-actin depolymerization was not responsible for the observed effects. For this we treated cells with 2 nM latrunculin B and stained their actin cytoskeleton. In Figure 9A we show representative control cells, contain-

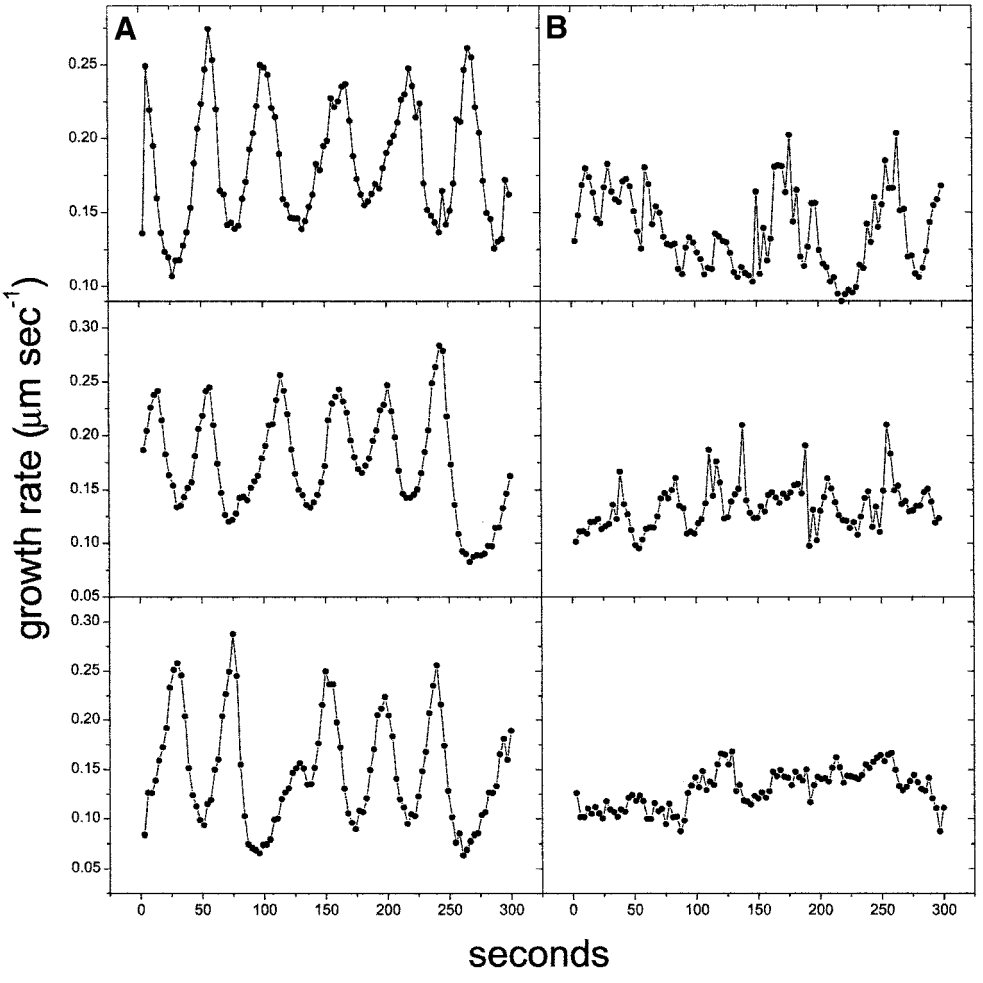

Figure 10. Effect of latrunculin B on the oscillatory growth of the pollen tube. (A) Growth rate profile for 5 min of three representative control cells. (B) Growth rate profile of three representative cells treated with 1 nM latrunculin B. Note that although the treated cells are still growing, their oscillatory pattern has been disrupted.

ing long oriented cables of actin in their shank, a disorganized meshwork in their apex and a prominent subapical aggregation of F-actin bundles in the form of a funnel (Figure 9A, arrow). This funnel-like structure occupies the base of the clear zone at the site where cytoplasmic streaming reverses direction. In the presence of 2 nM latrunculin B this structure is either absent or highly reduced (Figure 9B). The funnel-like structure is internal and does not appear to constitute a cortical ring as described in tobacco and maize pollen (Kost *et al.*, 1998; Gibbon *et al.*, 1999). A similar structure has been observed in poppy pollen tubes (Geitmann *et al.*, 2000). Our results suggest that this actin structure is important for the optimal growth of the pollen tube.

Because growing pollen tubes posses an oscillatory growth pattern (Pierson *et al.*, 1996), we tested the participation of the actin cytoskeleton in this phenomenon. The presence of only 1 nM latrunculin B in the medium abolished the oscillatory growth pattern in most of the cells analyzed (a total of 30, see Figure 10 for representative cells), suggesting that actin polymerization could participate in the oscillatory process. Inhibition of pulsatile growth, a process that could be related to the oscillations observed in *Lilium* pollen, has been observed in cytochalasin D–treated tobacco pollen tubes (Geitmann *et al.*, 1996). However, those observations were obscured by the fact that the cells were growing at only ~10% of their original rate, whereas in our analysis they were growing at ~75% the rate of the controls.

DISCUSSION

Our results show that profilin, DNAse I, latrunculin B, and cytochalasin D block pollen tube growth at a significantly lower concentration than that needed to inhibit cytoplasmic streaming. These observations disagree with the simplest hypothesis that actin participation in pollen tube growth is only needed for the transport of secretory vesicles to the tip (Mascarenhas and Lafountain, 1972; Mascarenhas, 1993; Taylor and Hepler, 1997; Kost *et al.*, 1998; Geitmann and Emons, 2000) and suggest instead that actin polymerization is rate limiting for pollen tube elongation.

These results suggest a possible scenario for the dynamic state of the actin cytoskeleton in the pollen tube. We hypothesize that monomers are rapidly incorporated into the barbed-end of filaments from the actin–profilin complex and that the filaments are subsequently barbed-end capped and incorporated into the longitudinal bundles present in the rest of the cell. In this scheme, the inhibition of pollen tube

growth by excess profilin as well as by DNAse I and latrunculin B will be due to a block of regulated nucleation. Furthermore, DNAse I and latrunculin B should also inhibit filament elongation from profilin–actin complexes. These two molecules can probably bind actin in the presence of profilin, because their binding sites on actin are opposite to the profilin binding site (Kabsch *et al.*, 1990; Schutt *et al.*, 1993; Morton *et al.*, 2000; Yarmola *et al.*, 2000). Note that latrunculin B is active at very low concentrations because it is cell permeant and is present in the culture chamber at a large excess over actin; hence the free latrunculin B concentration does not change in the cell, whereas the latrunculin-actin complex can reach the inhibitory level. The higher concentration of profilin needed to block growth may be due to a lower affinity for actin (Gibbon *et al.*, 1997) and due to the fact that it will not block filament elongation (Perelroizen *et al.*, 1996; Kang *et al.*, 1999).

The inhibition of streaming will be caused by the shortening of the filaments that compose a bundle due to the sequestering of subunits from barbed-end capped filaments. If both ends were free, profilin should have only a minor depolymerizing effect on the microfilaments (Perelroizen *et al.*, 1996). In other plant cells, excess profilin has been repeatedly shown to have a strong depolymerizing effect (Staiger *et al.*, 1994; Holzinger *et al.*, 1997; Valster *et al.*, 1997), further supporting the conclusion that the microfilaments in the pollen tube have their barbed-end capped. The effect of cytochalasin D on cytoplasmic streaming is probably not due to depolymerization of microfilaments but to the previously documented rearrangement of the actin cytoskeleton (Lancelle and Hepler, 1988; Tang *et al.*, 1989).

In previous studies in pollen tubes (Gibbon *et al.*, 1999; Geitmann *et al.*, 2000) and root hairs (Miller *et al.*, 1999), it has been observed that cytoplasmic streaming continues in cells that are not elongating after latrunculin B or cytochalasin D treatment, but no effort to quantitate these rates was made. Based partially on this observation the investigators suggested the existence of a highly dynamic apical population of F-actin, necessary for growth, that is sensitive to depolymerization or stabilization and independent of cytoplasmic streaming. Our results support this hypothesis by quantitatively demonstrating that the function of actin polymerization is independent of vesicle transport. Nevertheless, our results do not rule out the possibility that the inhibited step is actin-dependent secretion.

It is well known that cytosolic calcium is high at the extreme tip of the pollen tube, creating a gradient that is necessary for pollen tube elongation (Pierson *et al.*, 1994). Also, small Rho-type GTPases (Rops in plants) have been localized to the tip membrane of growing pollen tubes (Lin *et al.*, 1996; Kost *et al.*, 1999), and they have been found to have pronounced effects on polarity maintenance (Kost *et al.*, 1999) and growth (Lin and Yang, 1997). Furthermore, Rops probably act in a common pathway with PIP_2 (Kost *et al.*, 1999) and calcium (Li *et al.*, 1999) to regulate pollen tube elongation via their control of actin polymerization (Fu *et al.*, 2001). Based on the similarity of components, it seems likely that a mechanism related to the one operating in animal and yeast cells could nucleate new microfilaments in pollen tubes. This will require that signals are transduced from Rop and PIP_2 to the plant homologue of the Arp2/3 complex, as in animals and yeast (Machesky and Gould, 1999). Interestingly, pollen tube growth rates in culture match closely the velocity of *Listeria* motility in vitro and in animal cells (Theriot *et al.*, 1992; Loisel *et al.*, 1999), a process well known to be dependent on actin nucleation and polymerization (Cameron *et al.*, 1999; Loisel *et al.*, 1999). Furthermore, concentrations of profilin above the optimal inhibit polymerization-based bacterial motility in vitro (Loisel *et al.*, 1999), and high profilin concentrations can reduce Arp2/3 complex–induced polymerization (Machesky *et al.*, 1999; Yang *et al.*, 2000).

Pollen tubes growing in the presence of 2 nM latrunculin B grow erratically and with a very reduced clear zone. The main difference in their actin cytoskeleton with control cells is a drastic reduction or complete absence of a subapical funnel-shaped F-actin array (Figure 9). The position of this funnel-like structure overlaps with a recently described alkaline band present in *Lilium* pollen tubes that occupies the base of the clear zone (Feijó *et al.*, 1999), and the region where cytoplasmic streaming lanes reverse direction. We further suggest that in this region the rapidly formed microfilaments become incorporated into bundles, by the action of recently described villin (Vidali *et al.*, 1999). Additionally, activation of the severing activity of ADF by the high pH at this region could generate new barbed-ends and the formation of more F-actin.

In summary, our results indicate that actin polymerization and stability, independently from cytoplasmic streaming, are essential for pollen tube growth. Although the detailed mechanism for the participation of actin in pollen tube growth still remains to be elucidated, the present quantitative approach establishes a framework for future experimentation

ACKNOWLEDGMENTS

We thank Dr. Federico Sánchez (Instituto de Biotecnología, UNAM) for his support and Dr, Steven Almo (Albert Einstein College of Medicine) for the kind donation of the human profilin 1 clone. The lily bulbs were donated by Fred C. Gloeckner and Co. (Harrison, NY). We also thank Mr. Ronald Beckwith and Ms. Monika Johnson for growing the plants and Dr. Terena Holdaway-Clarke and Mr. Grant Hackett for their important support in computer matters. This work was supported by National Science Foundation grants MCB-9601087 and MCB-0077599 to P.K.H. and a Doctoral fellowship from DGAPA, UNAM Mexico to L.V.

REFERENCES

Ayscough, K.R., Stryker, J., Pokala, N., Sanders, M., Crews, P., and Drubin, D.G. (1997). High rates of actin filament turnover in budding yeast and roles for actin in establishment and maintenance of cell polarity revealed using the actin inhibitor latrunculin-A. J. Cell Biol. *137*, 399–416.

Cameron, L.A., Footer, M.J., van Oudenaarden, A., and Theriot, J.A. (1999). Motility of ActA protein-coated microspheres driven by actin polymerization. Proc. Natl. Acad. Sci. USA *96*, 4908–4913.

Carter, L.K., Christopherson, R.I., and dos Remedios, C. G. (1997). Analysis of the binding of deoxyribonuclease I to G-actin by capillary electrophoresis. Electrophoresis *18*, 1054–1058.

Coue, M., Brenner, S.L., Spector, I., and Korn, E.D. (1987). Inhibition of actin polymerization by latrunculin A. FEBS Lett. *213*, 316–318.

de Win, A.H.N. (1997). Quantitative analysis of organelle movements in pollen tubes. Ph.D. thesis. Nijmegen University, The Netherlands.

Derksen, J., Rutten, T., van Amstel, T., de Win, A., Doris, F., and Steer, M. (1995). Regulation of pollen tube growth. Acta Bot. Neerl. *44*, 93–119.

Doris, F.P., and Steer, M.W. (1996). Effects of fixatives and permeabilization buffers on pollen tubes: implications for localization of actin microfilaments using phalloidin staining. Protoplasma *195*, 25–36.

Fedorov, A.A., Pollard, T.D., and Almo, S.C. (1994). Purification, characterization and crystallization of human platelet profilin expressed in *Escherichia coli*. J. Mol. Biol. *241*, 480–482.

Feijó, J.A., Sainhas, J., Hackett, G.R., Kunkel, J.G., and Hepler, P.K. (1999). Growing pollen tubes possess a constitutive alkaline band in the clear zone and a growth-dependent acidic tip. J. Cell Biol. *144*, 483–496.

Franke, W.W., Herth, W., VanDerWoude, W.J., and Morre, D.J. (1972). Tubular and filamentous structures in pollen tubes: possible involvement as guide elements in protoplasmic streaming and vectorial migration of secretory vesicles. Planta *105*, 317–341.

Fu, Y., Wu, G., and Yang, Z.B. (2001). Rop GTPase-dependent dynamics of tip-localized F-actin controls tip growth in pollen tubes. J. Cell Biol. *152*, 1019–1032.

Geitmann, A., and Emons, A.M. (2000). The cytoskeleton in plant and fungal cell tip growth. J. Microsc. *198*, 218–245.

Geitmann, A., Li, Y.Q., and Cresti, M. (1996). The role of the cytoskeleton and dictyosome activity in the pulsatory growth of *Nicotiana tabacum* and *Petunia hybrida* pollen tubes. Bot. Acta *109*, 102–109.

Geitmann, A., Snowman, B.N., Emons, A.M.C., and Franklin-Tong, V.E. (2000). Alterations in the actin cytoskeleton of pollen tubes are induced by the self-incompatibility reaction in *Papaver rhoeas*. Plant Cell *12*, 1239–1251.

Gibbon, B.C., Kovar, D.R., and Staiger, C.J. (1999). Latrunculin B has different effects on pollen germination and tube growth. Plant Cell *11*, 2349–2363.

Gibbon, B.C., Ren, H., and Staiger, C.J. (1997). Characterization of maize (*Zea mays*) pollen profilin function in vitro and in live cells. Biochem. J. *327*, 909–915.

Gupta, G.D., and Heath, I.B. (1997). Actin disruption by latrunculin B causes turgor-related changes in tip growth of *Saprolegnia ferax* hyphae. Fungal Gen. Biol. *21*, 64–75.

Heslop-Harrison, J., and Heslop-Harrison, Y. (1990). Dynamic aspects of apical zonation in the angiosperm pollen tube. Sex. Plant Reprod. *3*, 187–194.

Heslop-Harrison, J., and Heslop-Harrison, Y. (1991). The actin cytoskeleton in unfixed pollen tubes following microwave-accelerated DMSO-permeabilization and TRITC-phalloidin staining. Sex Plant Reprod. *4*, 6–11.

Holzinger, A., Mittermann, I., Laffer, S., Valenta, R., and Meindl, U. (1997). Microinjection of profilins from different sources into the green alga micrasterias causes transient inhibition of cell growth. Protoplasma *199*, 124–134.

Kabsch, W., Mannherz, H.G., Suck, D., Pai, E.F., and Holmes, K.C. (1990). Atomic structure of the actin:DNase I complex. Nature *347*, 37–44.

Kang, F., Purich, D.L., and Southwick, F.S. (1999). Profilin promotes barbed-end actin filament assembly without lowering the critical concentration. J. Biol. Chem. *274*, 36963–36972.

Kost, B., Lemichez, E., Spielhofer, P., Hong, Y., Tolias, K., Carpenter, C., and Chua, N.H. (1999). Rac homologues and compartmentalized phosphatidylinositol 4,5- bisphosphate act in a common pathway to regulate polar pollen tube growth. J. Cell Biol. *145*, 317–330.

Kost, B., Spielhofer, P., and Chua, N.H. (1998). A GFP-mouse talin fusion protein labels plant actin filaments in vivo and visualizes the actin cytoskeleton in growing pollen tubes. Plant J. *16*, 393–401.

Kovar, D.R., Drobak, B.K., and Staiger, C.J. (2000). Maize profilin isoforms are functionally distinct. Plant Cell *12*, 583–598.

Lancelle, S.A., Cresti, M., and Hepler, P.K. (1987). Ultrastructure of the cytoskeleton in freeze-substituted pollen tubes of *Nicotiana alata*. Protoplasma *140*, 141–150.

Lancelle, S.A., and Hepler, P.K. (1988). Cytochalasin-induced ultrastructural alterations in *Nicotiana* pollen tubes. Protoplasma Suppl. *2*, 65–75.

Lancelle, S.A., and Hepler, P.K. (1992). Ultrastructure of freeze-substituted pollen tubes of *Lilium longiflorum*. Protoplasma *167*, 215–230.

Lazarides, E., and Lindberg, U. (1974). Actin is the naturally occurring inhibitor of deoxyribonuclease I. Proc. Natl. Acad. Sci. USA *71*, 4742–4746.

Li, H., Lin, Y., Heath, R.M., Zhu, M.X., and Yang, Z. (1999). Control of pollen tube tip growth by a Rop GTPase-dependent pathway that leads to tip-localized calcium influx. Plant Cell *11*, 1731–1742.

Lin, Y., Wang, Y., Zhu, J.K., and Yang, Z. (1996). Localization of a Rho GTPase implies a role in tip growth and movement of the generative cell in pollen tubes. Plant Cell *8*, 293–303.

Lin, Y., and Yang, Z. (1997). Inhibition of pollen tube elongation by microinjected anti-Rop1Ps antibodies suggests a crucial role for Rho-type GTPases in the control of tip growth. Plant Cell *9*, 1647–1659.

Loisel, T.P., Boujemaa, R., Pantaloni, D., and Carlier, M.F. (1999). Reconstitution of actin-based motility of *Listeria* and *Shigella* using pure proteins. Nature *401*, 613–616.

Machesky, L.M., and Gould, K.L. (1999). The Arp2/3 complex: a multifunctional actin organizer. Curr. Opin. Cell Biol. *11*, 117–121.

Machesky, L.M., Mullins, R.D., Higgs, H.N., Kaiser, D.A., Blanchoin, L., May, R.C., Hall, M.E., and Pollard, T.D. (1999). Scar, a WASp-related protein, activates nucleation of actin filaments by the Arp2/3 complex. Proc. Natl. Acad. Sci. USA *96*, 3739–3744.

Mascarenhas, J.P. (1993). Molecular mechanisms of pollen tube growth and differentiation. Plant Cell *5*, 1303–1314.

Mascarenhas, J.P., and Lafountain, J. (1972). Protoplasmic streaming, cytochalasin B, and growth of the pollen tube. Tissue Cell *4*, 11–14.

Miller, D.D., de Ruijter, N.C.A., Bisseling, T., and Emons, A.M.C. (1999). The role of actin in root hair morphogenesis: studies with lipochito-oligosaccharide as a growth stimulator and cytochalasin as an actin perturbing drug. Plant J. *17*, 141–154.

Miller, D.D., Lancelle, S.A., and Hepler, P.K. (1996). Actin microfilaments do not form a dense meshwork in *Lilium longiflorum* pollen tube tips. Protoplasma *195*, 123–132.

Morton, W.M., Ayscough, K.R., and McLaughlin, P.J. (2000). Latrunculin alters the actin-monomer subunit interface to prevent polymerization. Nat. Cell Biol. *2*, 376–378.

Oliveira, C.A., Chedraoui, S., and Mantovani, B. (1997). Latrunculin A is a potent inducer of aggregation of polymorphonuclear leukocytes. Life Sci. *61*, 603–609.

Perdue, T.D., and Parthasarathy, M.V. (1985). In situ localization of F-actin in pollen tubes. Eur. J. Cell Biol. *39*, 13–20.

Perelroizen, I., Didry, D., Christensen, H., Chua, N.H., and Carlier, M.F. (1996). Role of nucleotide exchange and hydrolysis in the function of profilin in action assembly. J. Biol. Chem. *271*, 12302–12309.

Picton, J.M., and Steer, M.W. (1982). A model for the mechanism of tip extension in pollen tubes. J. Theor. Biol. *98*, 15–20.

Pierson, E.S., Miller, D.D., Callaham, D.A., Shipley, A.M., Rivers, B.A., Cresti, M., and Hepler, P.K. (1994). Pollen tube growth is coupled to the extracellular calcium ion flux and the intracellular calcium gradient: effect of BAPTA-type buffers and hypertonic media. Plant Cell *6*, 1815–28.

Pierson, E.S., Miller, D.D., Callaham, D.A., van Aken, J., Hackett, G., and Hepler, P.K. (1996). Tip-localized calcium entry fluctuates during pollen tube growth. Devel. Biol. *174*, 160–173.

Pollard, T.D., Blanchoin, L., and Mullins, R.D. (2000). Molecular mechanisms controlling actin filament dynamics in nonmuscle cells. Annu. Rev. Biophys. Biomol. Struct. *29*, 545–576.

Sampath, P., and Pollard, T.D. (1991). Effects of cytochalasin, phalloidin, and pH on the elongation of actin filaments. Biochemistry *30*, 1973–1980.

Schatten, G., Schatten, H., Spector, I., Cline, C., Paweletz, N., Simerly, C., and Petzelt, C. (1986). Latrunculin inhibits the microfilament-mediated processes during fertilization, cleavage and early development in sea urchins and mice. Exp. Cell Res. *166*, 191–208.

Schutt, C.E., Myslik, J.C., Rozycki, M.D., Goonesekere, N.C., and Lindberg, U. (1993). The structure of crystalline profilin-beta-actin. Nature *365*, 810–816.

Shimmen, T., and Yokota, E. (1994). Physiological and biochemical aspects of cytoplasmic streaming. Int. Rev. Cytol. *155*.

Staiger, C.J., Yuan, M., Valenta, R., Shaw, P.J., Warn, R.M., and Lloyd, C.W. (1994). Microinjected profilin affects cytoplasmic streaming in plant cells by rapidly depolymerizing actin microfilaments. Curr. Biol. *4*, 215–219.

Steer, M.W., and Steer, J.M. (1989). Pollen tube tip growth. New Phytol. *111*, 323–358.

Tang, X.J., Lancelle, S.A., and Hepler, P.K. (1989). Fluorescence microscopic localization of actin in pollen tubes: comparison of actin antibody and phalloidin staining. Cell Motil. Cytoskeleton *12*, 216–24.

Taylor, L.P., and Hepler, P.K. (1997). Pollen germination and tube growth. Ann. Rev. Plant Physiol. Plant Mol. Biol. *48*, 461–491.

Theriot, J.A., Mitchison, T.J., Tilney, L.G., and Portnoy, D.A. (1992). The rate of actin-based motility of intracellular *Listeria monocytogenes* equals the rate of actin polymerization. Nature *357*, 257–260.

Valster, A.H., Pierson, E.S., Valenta, R., Hepler, P.K., and Emons, A.M. (1997). Probing the plant actin cytoskeleton during cytokinesis and interphase by profilin microinjection. Plant Cell *9*, 1815–1824.

Vidali, L., and Hepler, P.K. (1997). Characterization and localization of profilin in pollen grains and tubes of *Lilium longiflorum*. Cell Motil. Cytoskeleton *36*, 323–338.

Vidali, L., and Hepler, P.K. (2000). Actin in pollen and pollen tubes. In: Actin: A Dynamic Framework for Multiple Plant Cell Functions, ed. C. J. Staiger, F. Baluska, D. Volkmann, and P. Barlow, Dordrecht, The Netherlands: Kluwer Academic Publishers, 323–345.

Vidali, L., and Hepler, P.K. (2001). Actin and pollen tube growth. Protoplasma *215*, 64–76.

Vidali, L., Yokota, E., Cheung, A.Y., Shimmen, T., and Hepler, P.K. (1999). The 135 kDa actin-bundling protein from *Lilium longiflorum* pollen is the plant homologue of villin. Protoplasma *209*, 283–291.

Yang, C.S., Huang, M.Z., DeBiasio, J., Pring, M., Joyce, M., Miki, H., Takenawa, T., and Zigmond, S.H. (2000). Profilin enhances Cdc42-induced nucleation of actin polymerization. J. Cell Biol. *150*, 1001–1012.

Yarmola, E.G., Somasundaram, T., Boring, T.A., Spector, I., and Bubb, M.R. (2000). Actin-latrunculin. A structure and function—differential modulation of actin-binding protein function by latrunculin A. J. Biol. Chem. *275*, 28120–28127.